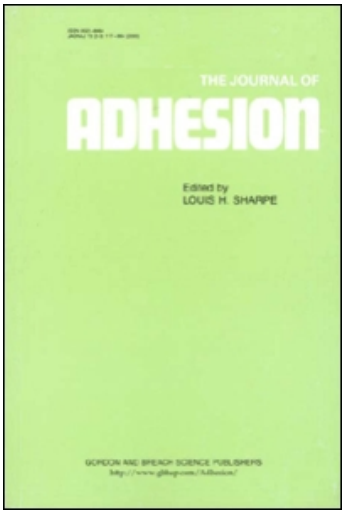

The Journal of Adhesion
Publication details, including instructions for authors and subscription information:
http://www.informaworld.com/smpp/title~content=t713453635

Study of the Interfacial Reaction of Styrene/Maleic Anhydride Copolymerand (Amine)-Terminated Butadiene-Acrylonitrile Copolymer Using FTIR Imaging Techniques

Eun-Mi Shin[a]; Jack L. Koenig[a]
[a] Department of Macromolecular Science & Engineering, Case Western Reserve University, Cleveland, Ohio, USA

Online publication date: 08 September 2010

To cite this Article Shin, Eun-Mi and Koenig, Jack L.(2002) 'Study of the Interfacial Reaction of Styrene/Maleic Anhydride Copolymerand (Amine)-Terminated Butadiene-Acrylonitrile Copolymer Using FTIR Imaging Techniques', The Journal of Adhesion, 78: 10, 877 — 894
To link to this Article: DOI: 10.1080/00218460214098
URL: http://dx.doi.org/10.1080/00218460214098

The Journal of Adhesion, 78: 877–894, 2002

0021-8464/02 $12.00 +.00
DOI: 10.1080/00218460290010485

STUDY OF THE INTERFACIAL REACTION OF STYRENE/MALEIC ANHYDRIDE COPOLYMER AND (AMINE)-TERMINATED BUTADIENE-ACRYLONITRILE COPOLYMER USING FTIR IMAGING TECHNIQUES

Eun-Mi Shin
Jack L. Koenig
Department of Macromolecular Science & Engineering,
Case Western Reserve University,
Cleveland Ohio, USA

The interfacial reaction between styrene/maleic anhydride copolymer (SMA) and amine-terminated butadiene-acrylonitrile copolymer (ATBA) was observed using Fourier transform infrared (FTIR) imaging spectroscopy. The anhydride and amine reacted to form an imide. Each component was detected using a characteristic wavenumber, which was 1601 cm^{-1} for SMA, 2237 cm^{-1} for ATBA, and 1701 cm^{-1} for the imide. FTIR images were taken as the reaction proceeded at 150, 160, 170, and 180°C. At low temperatures (150 and 160°C), diffusion-controlled kinetics were observed since interdiffusion between the reactants did not appear in the images. On the other hand, both the diffusion front and the reaction front are observed in the images at high reaction temperatures (170 and 180°C), which indicates that the kinetics became reaction-controlled rather than diffusion-controlled. Absorbance profiles were extracted from the images and used for the calculation of the extent of reaction. The data were analyzed using the Frederickson and Milner theory based on the assumption of diffusion-controlled kinetics, and this theory fit the low reaction temperature data.

Keywords: FTIR imaging; Interfacial reaction; Interdiffusion; Diffusion-controlled kinetics; Reaction-controlled kinetics; Interface instability

Received 16 October 2001; in final form 15 April 2002.

This is one of a collection of papers honoring Hatsuo (Ken) Ishida, the recipient in February 2001 of *The Adhesion Society Award for Excellence in Adhesion Science, Sponsored by 3M*.

Address correspondence to Jack L. Koenig, Department of Macromolecular Science & Engineering, Case Western Reserve University, 10900 Euclid Avenue, Cleveland, OH 44106-7202. E-mail: jlk6@po.cwru.edu

INTRODUCTION

The process of adhesion is significant in a variety of applications including polymer blends, coatings, and adhesives on or between thermoplastics. There have been a few studies of the interdiffusion of two miscible polymers [1] and interfacial reactions between functionalized polymers [2]. The main goal of the interdiffusion and interfacial reactions is better adhesion between two polymers.

There are only a few miscible polymer blends with commercial applications. By far, most polymer blends used on the industrial scale are heterogeneous systems [3]. Thus, for completely immiscible systems, the question of compatibilization arises. The main goal of compatibilization is improved interfacial adhesion, which can be achieved by adding preformed block copolymers [4–6] or by reactive blending [7–9]. Reactive blending is an important and increasingly accepted method for the compatibilization of polymer blends. Two or more immiscible polymeric components are functionalized with chemical units, which are coreactive. During melt processing, the polymers chemically react to form a copolymer at the interface between the two phases. This copolymer reduces the interfacial tension between the two phases, provides for better dispersion, and promotes adhesion between the phases. The kinetics and extent of reaction between the functionalized polymers are critical parameters in determining reactive blend properties.

Frederickson [10], Frederickson and Milner [11], and O'Shaughnessy and Sawhney [12, 13] have made theoretical analyses of polymer-polymer interfacial reactions independently. It was assumed in both treatments that the chains are symmetric in size, that a flat interface is formed between them under quiescent conditions, and that reactive groups are located at the end of each chain. Their theoretical studies predicted that the interfacial reaction kinetics could be divided into three different time regimes with the assumption that diffusion controls the overall reaction kinetics. On the other hand, Oyama and Inoue [14] analyzed interfacial reactions between end-functionalized polymers [16, 21–23] and concluded that the reaction rate controlled the overall reaction kinetics.

In general, rather little extent of reaction is necessary during reactive compatabilization to create a substantial change in morphology or physical properties [15–18]. However, it can be difficult to determine either the rate of reaction or the amount of copolymer formed in such experiments. The reactive polymers in these studies are typically heterogeneous in both degree of functionality and molecular weight. Highly functionalized polymers can form densely grafted copolymers or even cross-linked structures at the interface.

Nuclear magnetic resonance (NMR) [19, 20] and size exclusion chromatography (SEC) [9, 21, 22] have been used to measure the extent of reaction in the final blend. Infrared spectroscopy [23] and FTIR microscopy [24] were used on reactive blends to follow the reaction kinetics and to detect the interdiffusion at the polymer interfaces. Schulze *et al.* [22, 25] used forward recoil spectroscopy (FRES) to measure the extent of reaction and kinetics as well as concentration profiles of the reactants. These methods usually take considerable time and sometimes require complicated mathematics after the measurements to determine the extent of the reactions.

Recently, a new infrared imaging technique has emerged which utilizes a focal plane array (FPA) detector coupled with a FTIR spectrometer to produce spatially resolved infrared spectral information [26]. This so-called fast FTIR imaging is unlike the previous step-and-collect or mapping experiments. Rather, it is a true imaging technique, acquiring both spatial and spectral information simultaneously. Compared with the step-and-collect mapping experiment, fast FTIR imaging acquires spectral information from large area in a short period of time. Therefore, one can get spectral and spatial information *in situ*. For this reason, the technique has been used for *in situ* analysis in solvent diffusion [27] and polymer dissolution experiments [28].

Using the fast FTIR technique in an interfacial reaction experiment yields many advantages. Spectral information gives kinetic data following functional groups, and spatially resolved spectral information gives diffusion data for both polymers. Figure 1 shows a schematic of the images that could appear as the interfacial reaction is controlled by either diffusion or reaction rate. Since FTIR imaging spectroscopy can resolve both chemical and spatial information simultaneously, it is possible for us to determine if the reaction kinetics were controlled by reaction rate or diffusion. In this work, we have used fast FTIR imaging spectroscopy to measure the extent of reaction at the styrene/maleic anhydride copolymer (SMA)/amine-terminated butadiene-acrylonitrile copolymer (ATBA) interface.

EXPERIMENTAL

Materials

All the chemicals used in this experiment were from Aldrich (Milwaukee, WI) and used as received. The SMA (Mw = 200,000) had maleic anhydride content of 14 wt%. The ATBA (amine equivalent weight = 900) had acrylonitrile content of 18 wt%. Toluene was used as a solvent.

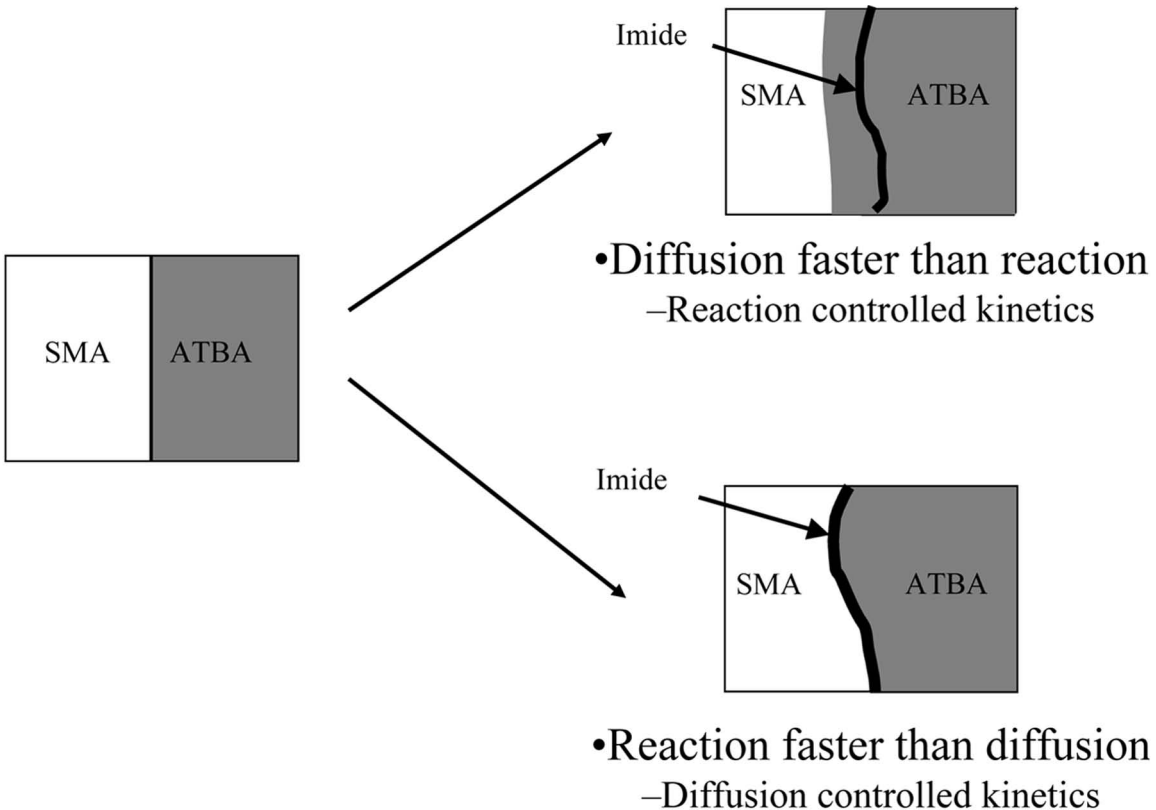

FIGURE 1 Cartoons of diffusion-controlled and reaction-controlled kinetics.

Sample Preparation

For FTIR monitoring of the bulk reaction, well-mixed samples of SMA/ATBA system were prepared. Toluene solutions (5 wt%) of SMA and ATBA were first prepared. These solutions were then quickly mixed stoichiometrically (one anhydride per one amine) to form homogeneous solutions. The stoichiometric mixtures were cast on a CaF_2 plate and dried at room temperature for one day. Then the cast sample was covered with another CaF_2 plate and the experiment was run.

For FTIR imaging, the SMA 5 wt% toluene solution was cast onto a CaF_2 plate and dried at room temperature. Then a 10 μm spacer was placed beside the SMA area on the CaF_2 plate and the sample was covered with another CaF_2 plate. The sandwiched SMA was annealed at 140°C to make a thin film. After the sandwich had cooled to room temperature, the viscous ATBA was introduced and diffused to make contact with the SMA film. The reaction temperatures were 150, 160, 170, and 180°C.

FTIR Spectroscopy and Fast FTIR Imaging

Infrared spectra were obtained using a Bio-Rad FTS-6000 in the kinetics mode for bulk reactions. The well-mixed samples were put on a hot stage (Mettler FP84HT with microscopy cell) and heated to a reaction temperature (150, 160, 170, and 180°C). Then spectra were collected every minute for at least 3 hours at a resolution of 4 cm^{-1}.

The Bio-Rad FTS6000 Stingray imaging spectrometer was used to acquire the infrared images. It consists of a step-scan interferometer bench (FTS6000) coupled to a Focal Plane Array (FPA) detector-equipped microscope, UMA-500 (Bio-Rad Laboratories, 237 Putnam Avenue, Cambridge, MA, USA). The microscope detector is a Mercury Cadmium Telluride (MCT) array of 64 × 64 elements imaging a spatial area of approximately 400 μm × 400 μm in a single data collection. The spatial resolution of the image was estimated as 6.25 μm from the dimensions and pixel number. To get a FTIR image of the interfacial reactions, a sandwiched sample was put on a different hot stage (Oxford Instrument [Concord, MA] with cryostat) and heated to the reaction temperature. The sample was kept at the reaction temperature for a certain time and then cooled to room temperature in order to collect the FTIR image. The time at which the sample was at the reaction temperature was considered to be the reaction time. The heat-up and cool-down time was excluded from the calculation of the comparative reaction times. The FTIR images were acquired at a resolution of 8 cm^{-1}. The acquisition time was 3.5 min per image. Image

acquisition and processing were carried out using Win-IR Pro and ENVI software. The area measurement under the peak of the imide profile was done using GRAMS (from Galactic) software integration function.

RESULTS AND DISCUSSION

The neat ATBA and SMA spectra are shown in Figure 2. Characteristic IR bands were selected to represent each component during the reaction. The C=C stretching band at 1601 cm^{-1} was selected for SMA and the peak at 2237 cm^{-1}, representing the C≡N stretching band, was used to characterize ATBA. The imide evolution was detected using the imide band at 1701 cm^{-1}.

Bulk reaction kinetics were obtained by heating a well-mixed sample to a reaction temperature. The growing imide peak can be seen as a function of time at 150°C in Figure 3a, where peak height was measured to calculate the relative amount of reaction. Spectra were taken every minute at 160, 170, and 180°C. Figure 3b shows the imide formation (% conversion) as a function of time for the different temperatures. The relative percent imide conversion was calculated as follows:

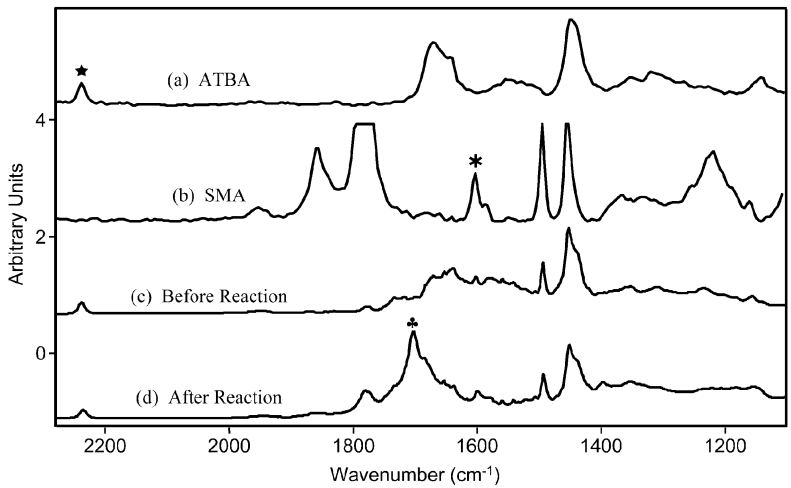

FIGURE 2 (a) Neat spectrum of ATBA. (b) Neat spectrum of SMA. (c) Spectrum of the well-mixed sample, before reaction. (d) Spectrum of after reaction at 180°C for 3 hours. ★, C≡N band represents ATBA at 2237 cm^{-1}; ∗, C=C band represents SMA at 1601 cm^{-1}; ♣, imide band at 1701 cm^{-1}.

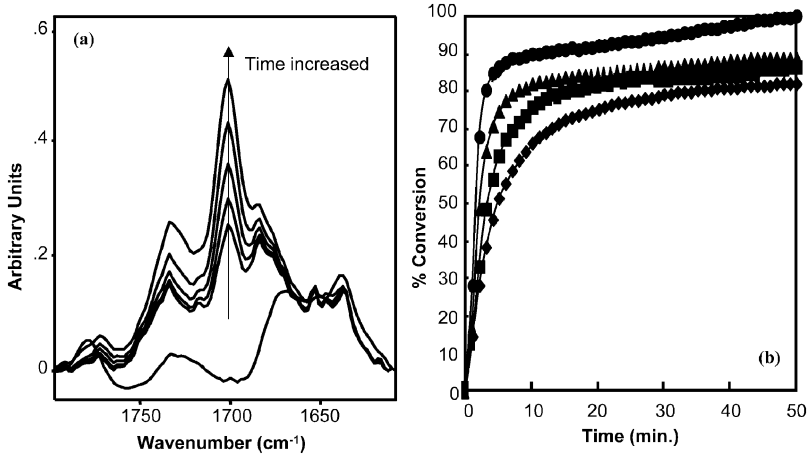

FIGURE 3 (a) Imide evolution with time at 150°C. (b) Percent conversion *versus* time for bulk reaction of SMA and ATBA at four different temperatures. ◆, 150°C; ■, 160°C; ▲, 170°C; ●, 180°C.

$$\text{Relative \% Conversion} = \{(I_{max} - I_t)/I_{max}\} \cdot 100, \qquad (1)$$

where I_{max} was the imide area calculated at the maximum and I_t was the peak area at a specific time. The amount of product increased rapidly at first and then reached at plateau, indicating that the reaction slowed significantly. This might be related to network formation, which hampers the diffusion of the components, or to the reaction being confined only to the region near the interface. The initial slope of the amount of product increased with temperature. The rate constant changed from $k = 24\ \text{min}^{-1}$ at 150°C to $k = 70\ \text{min}^{-1}$ at 180°C. An apparent activation energy obtained from an Arrhenius plot yielded a value of 52 kJ/mol. These values are comparable with previously reported values of the reaction of SMA with amine [24].

Images extracted using characteristic bands from the interfacial reaction at 160°C may be seen in Figure 4. Absorbance intensities of the images are thresholded to the values shown with the color bars. The red color represents relatively high intensity and the blue color relatively low intensity. The imide formation from the reaction of SMA and ATBA was seen clearly at the interface as the reaction proceeded. As the reaction proceeded the thickness of the imide strip in the images became wider and the red color became strong. The images of the SMA and ATBA show sharp interfaces even with long reaction time. The images of the interfacial reaction at 150°C showed that the same sharp interface as the imide was formed. If the diffusion rate is

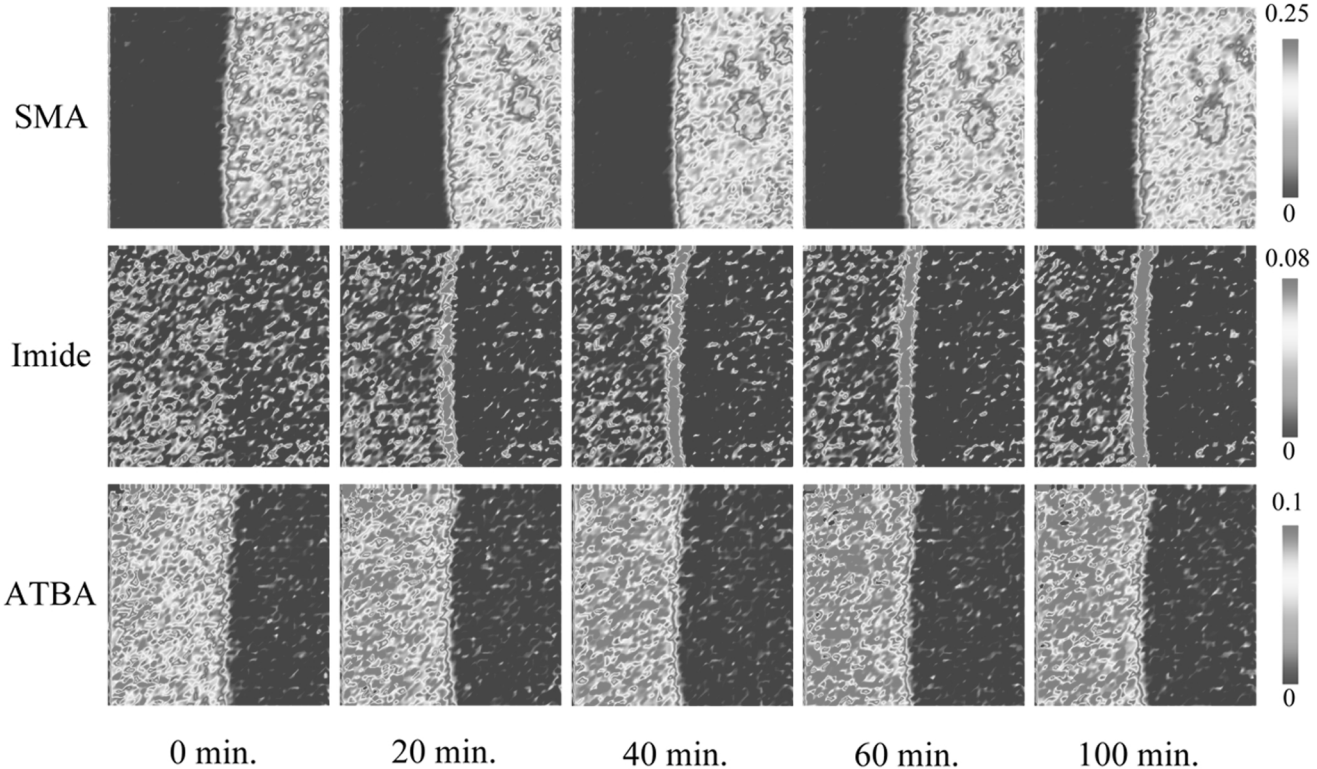

FIGURE 4 Absorbance images of SAM, ATBA, and imide. Reaction temperature was 160°C. Imide evolution was seen with time on the SAM/ATBA interface (see Color Plate I).

faster than the reaction rate, we should be able to see the diffusion by gradual color change between the two reactants in the images and the imide would form behind the diffusion front. The sharp interface (no gradual color change) with the imide formation at the interface leads us to conclude that the interfacial reaction of this particular system is a diffusion-controlled kinetic reaction.

Absorbance profiles for each of the components can be extracted from any row in the image, perpendicular to the interface. Figure 5 shows the typical absorbance profiles of SMA, ATBA, and imide evolution at the interface. Imide formation at the interface of SMA/ATBA, as the reaction progressed, can also be seen in the absorbance profiles by the peak of the imide profile that developed where the SMA and ATBA profiles crossed, which is the interface of SMA/ATBA.

The amount of imide formation was calculated using the area under the peak of the imide absorbance profiles. The scheme for the area measurement, and the imide evolution with time, are shown in Figure 6. Using the imide profile peak area and Equation (1), the interfacial reaction kinetics were plotted as percent conversion *versus* time (Figure 7). The rate constants were extracted from the initial slopes of the plots. The initial slope of the reaction increases with temperature and is proportional to the reaction rate constant. The rate constant changes from $k = 0.26\,\mathrm{min}^{-1}$ at 150°C to $k = 3.41\,\mathrm{min}^{-1}$ at 180°C from the percent conversion plots.The calculated interfacial reaction rate constants are shown in Table 1 compared with the rate constants for the bulk reactions. The activation energy was calculated by constructing an Arrhenius plot using the calculated rate constants. The Arrhenius equation is

$$\mathrm{Ln}(k) = \mathrm{Ln}(\mathrm{A}) - \mathrm{E_a}/\mathrm{RT}, \tag{2}$$

where A is the frequency factor, $\mathrm{E_a}$ is the activation energy, and R is the gas constant. The Arrhenius plots for both interfacial and bulk reaction are shown on Figure 8. The equations in Figure 8 are the linear fits to the data and the R^2 values. The activation energy calculated for the bulk reaction was 52 kJ/mol, and for interfacial reaction it was 133 kJ/mol.

Frederickson and Milner proposed a theory using three time regimes on the basis of the assumption that diffusion of the reactive chains controls the overall reaction kinetics [11]: (1) an initial regime, where the density of reactive chains in the interfacial region could be considered to be the same as the value in the bulk; (2) an intermediate regime, where there is a depletion hole of reactants in the interfacial region so that the reaction is controlled by diffusion of reactive

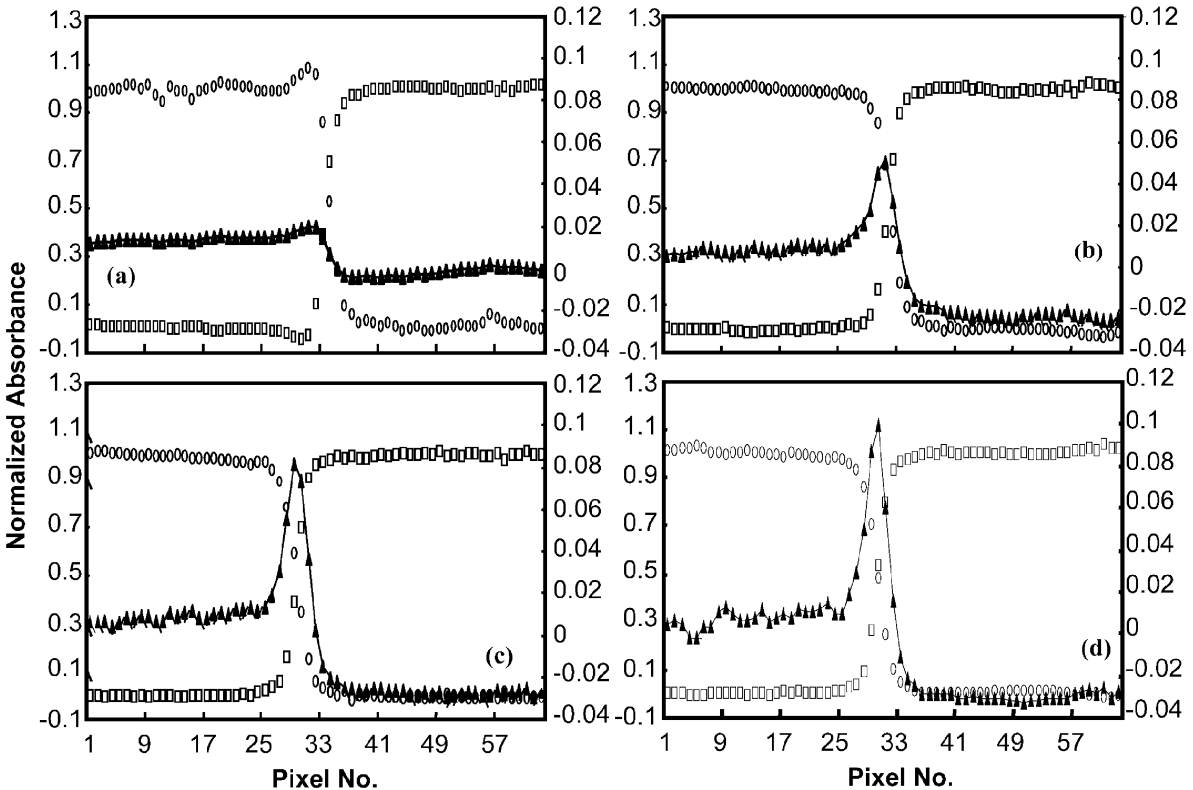

FIGURE 5 The absorbance profiles of ○, ATBA; □, SMA; and ▲, Imide at (a) 0 min, (b) 20 min, (c) 60 min, (d) 100 min. Reaction temperature was 160°C.

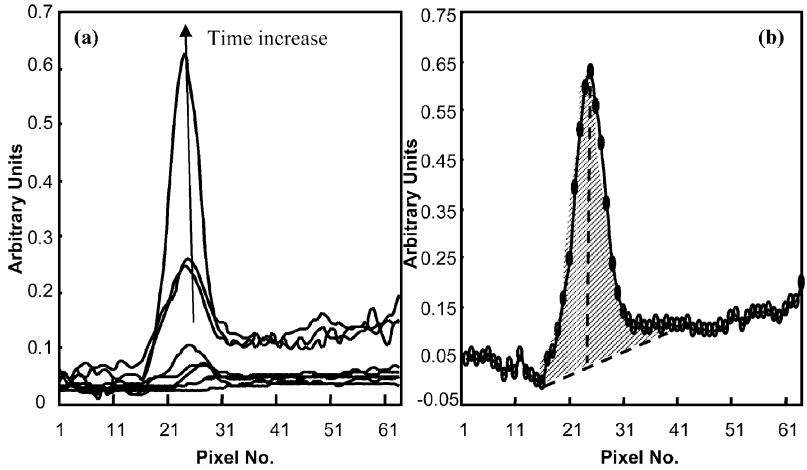

FIGURE 6 (a) Imide evolution with time at a reaction temperature of 150°C. (b) Area measurement under imide profile peak.

homopolymers to the interface; and (3) a late time regime, where interfacial saturation by the resultant copolymers suppressed the reaction. The predicted time dependence was a linear growth of the extent of reaction in time, t, a $t^{1/2}$ growth in the intermediate regime,

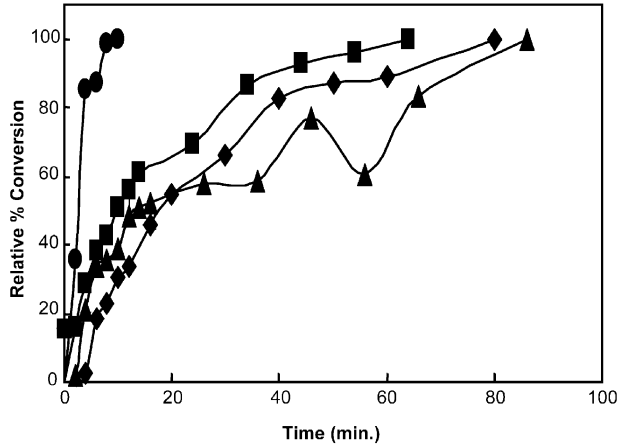

FIGURE 7 Percent conversion *versus* time for the interfacial reaction of SMA and ATBA at four different temperatures: ◆, 150°C; ■, 160°C; ▲, 170°C; and ●, 180°C.

TABLE 1 Rate Constants for Interfacial and for Bulk Reaction Obtained from Initial Slope of Reaction Kinetics

Temperature (°C)	$k_{\text{Interfacial reaction}}$	$k_{\text{Bulk reaction}}$
150	0.26	24
160	0.56	35
170	1.06	45
180	3.41	70

Unit of $k = \text{min}^{-1}$.

and a $(\ln t)^{1/2}$ growth in the late regime (Figure 9). Frederickson and Milner's theory has been applied to the relative percent conversion *versus* reaction time plot from FTIR imaging along with a linear regression analysis represented by R^2 values (Table 2). The R^2 values were over 0.99 at the early and intermediate regimes, indicating that the data fit the theory well at the early and the intermediate regimes. The R^2 value of the early time at 150°C was 1 since the fit was applied to only two data points. This was because there were not enough data points for the early regime at that reaction temperature. The well-fitted data prove again that this interfacial reaction followed diffusion-controlled kinetics.

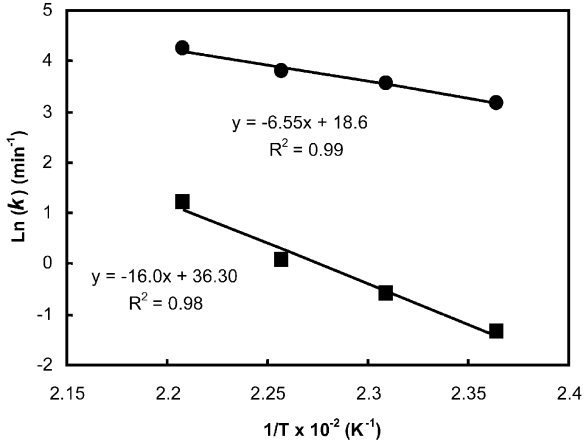

FIGURE 8 The Arrhenius plots of bulk (●) and interfacial (■) reaction. Lines are the linear regression fit to the data.

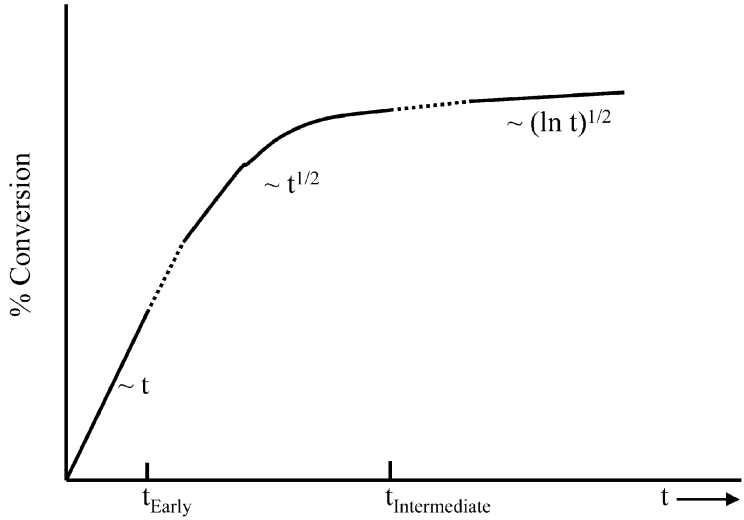

FIGURE 9 Qualitative summary of the time-dependent growth of percent conversion.

The R^2 value became less than 0.9 in the late regime at 170°C and the intermediate and late regimes for 180°C. Figure 10 shows the interface reaction images at 180°C and imide formation was observed inside the SMA phase at about 10 min. The ATBA images contain a separate strip of red beside the original interface apparent at the 10 min reaction time, which means that ATBA diffused into SMA so rapidly that the reaction could not keep up with the diffusion speed. The fast diffusion of ATBA can be seen more clearly in the absorbance profiles (Figure 11). The imide was formed on the interface

TABLE 2 R^2 Values from Linear Squared Fit of Frederickson's Theory to the Percent Conversion *versus* Time Plots

Temperature (°C)	Early regime ($\Sigma \propto t$)	Intermediate regime ($\Sigma \propto t^{1/2}$)	Late regime ($\Sigma \propto (\ln t)^{1/2}$)
150	1	0.9936	0.9365
160	0.9961	0.9903	0.9957
170	0.9863	0.9189	0.7349
180	0.9904	0.8839	0.7520

Σ represents percent conversion.

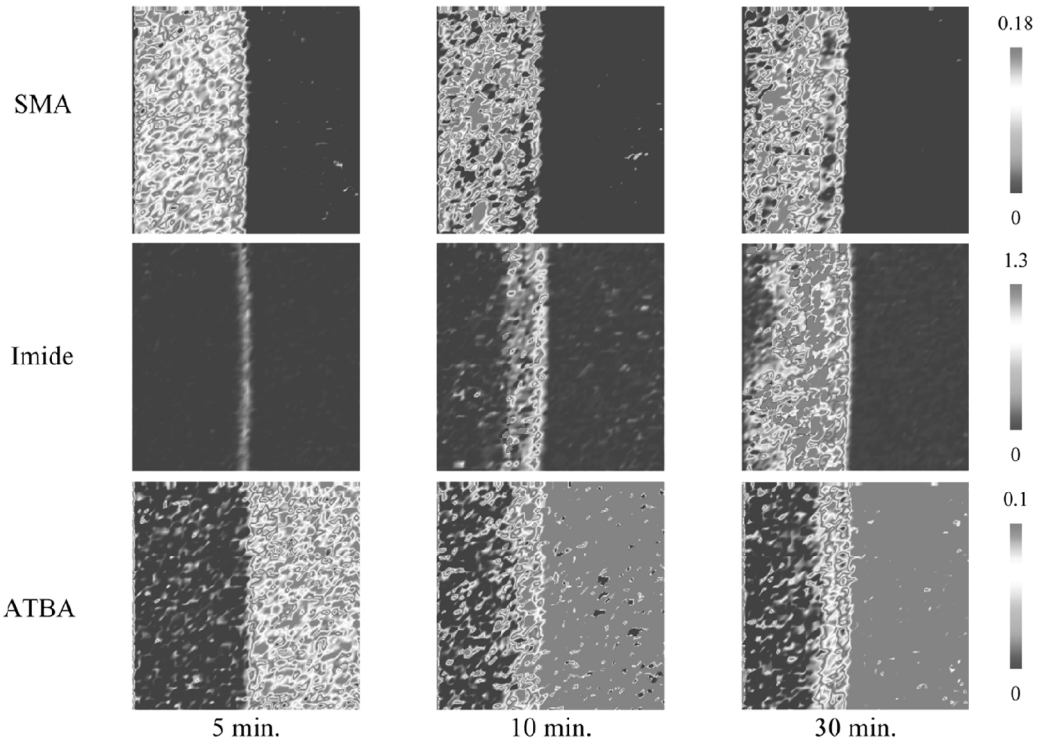

FIGURE 10 Absorbance images of SAM, ATBA, and imide. Reaction temperature was 180°C. Imide was formed at the SAM/ATBA interface and moved into SMA phase. ATBA diffusion formed another interface inside the SMA phase (see Color Plate II).

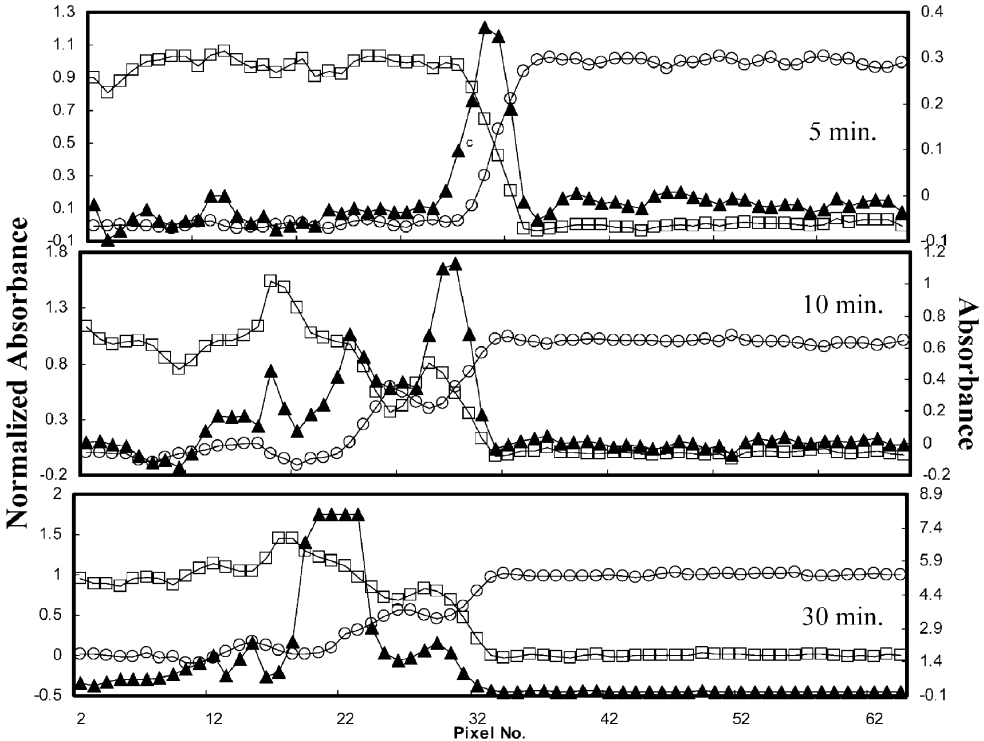

FIGURE 11 The absorbance profiles of ○, ATBA; □, SMA; and ▲, imide at 5 min, 10 min, and 30 min. Reaction temperature was 180°C.

of SMA/ATBA at 5 min and then broadened into the SMA phase at about 10 min. Shoulders of the ATBA and SMA profiles are inside of each other, revealing fast diffusion before reaction. At about 30 min, the highest peak of the imide profile moved into the SMA phase and a smaller imide profile peak formed on the shoulder part of the SMA and ATBA profiles. These observations show that the interface reaction kinetics changed from diffusion-controlled at low reaction temperatures to reaction-controlled at high reaction temperatures. The fact that the imide diffused to the SAM phase shows the interface instability. Therefore, Frederickson and Milner's theory [11] did not fit in the intermediate and late regimes at 170 and 180°C since the theory assumed a flat interface at quiescent conditions. It has been predicted that lower molecular weight copolymers will have a greater ability to reduce the interfacial tension at a given chemical potential or the extent of reaction [29]. Lower molecular weight copolymers are also more susceptible to thermal fluctuations, an observation that was used to explain the interfacial roughening observed in a Polystyrene (PS)/Poly(methyl methacrylate) (PMMA) reactive system [30]. Thus an interface saturated with low molecular weight copolymers, disrupted by both thermal fluctuations and a decrease in interfacial tension, may produce a higher extent of reaction. As the copolymer is added to a polymer-polymer interface, the interfacial tension is expected to decrease. If the interfacial tension is driven to zero, a microemulsion consisting of small droplets of one phase in the other, or a ribbed interface, may form between the two phases [31, 32]. In these experiments, the SMA has a very high molecular weight with the maleic anhydride moiety attached to a main chain, not at the end of the chain. The ATBA is a low molecular weight polymer with amine functionality at both ends. Therefore, the reaction may produce cross-links consisting of long main chains with low molecular weight bridges. Once copolymer and/or cross-links are formed, the interfacial tension decreases and the reactants can easily penetrate each other. Furthermore, because of the lowered interfacial tension and high reaction temperature, the mobility of the cross-linked polymer increases and it has a tendency to form one phase. Reduction of the interfacial tension has been the reason given for interfacial roughening observed in a similar reactive system [33].

CONCLUSIONS

We have obtained images of interfacial reactions using FTIR imaging. Using the measured absorbance profiles, we were able to calculate the amount of reaction at the interfaces. The FTIR images did not show

interdiffusion between the reactants at 150 and 160°C, with all the images showing sharp interfaces. The absorbance profiles at those reaction temperatures also showed a sharp interface, meaning that the reaction kinetics were diffusion controlled. At higher reaction temperatures, *i.e.*, 170 and 180°C, the images showed interdiffusion of the reactants and an interface instability. The interdiffusion and the interface instability can also be observed using absorbance profiles.

There were many benefits to using FTIR imaging spectroscopy to study interfacial reaction kinetics. Using FTIR imaging spectroscopy, one can monitor the interfacial reactions of the reacting components. Quantitative information can be obtained from absorbance profiles. In this study, we used only one system; therefore, we cannot draw global conclusions about the mechanism of interfacial reaction kinetics. Systematic studies with controlled molecular weight and with different functional groups are needed.

REFERENCES

[1] Sahlin, J. J. and Peppas, N. A., *Macromolecules*, **29**, 7124–7129 (1996).
[2] Lestriez, B., Chapel, J.-P. and Gérard, J.-F., *Macromolecules*, **34**, 1204–1213 (2001).
[3] Utracki, A. and Leszeck, A., *Polymer Alloys and Blends* (Hanser, Munich, Vienna, and New York, 1989).
[4] Auschra, C., Stadler, R. and Voigt-Martin, I. G., *Polymer*, **34**, 2081–2093 (1993).
[5] Shull, K. R. and Kramer, E. J., *Macromolecules*, **23**, 4769–4779 (1990).
[6] Braun, H., Rudolf, B. and Cantow, H.-J., *Poly. Bull.*, **32**, 241–248 (1994).
[7] Koning, C., Ikker, A., Borggreve, R., Leemans, L. and Moeller, M., *Polymer*, **34**, 4410–4416 (1993).
[8] Vermeesch, I. and Groeninckx, G., *J. Appl. Polym. Sci.*, **53**, 1365–1373 (1994).
[9] Guégan, P., Macosko, C. W., Ishizone, A. and Nakahama, S., *Macromolecules*, **27**, 4993–4997 (1994).
[10] Frederickson, G. H., *Phys. Rev. Lett.*, **76**, 3440–3445 (1996).
[11] Frederickson, G. H. and Milner, S. T., *Macromolecules*, **29**, 7386–7390 (1996).
[12] O'Shaughnessy, B. and Sawhney, U., *Phys. Rev. Lett.*, **76**, 3444–3447 (1996).
[13] O'Shaughnessy, B. and Sawhney, U., *Macromolecules*, **29**, 7230–7239 (1996).
[14] Oyama, H. T. and Inoue, T., *Macromolecules*, **34**, 3331–3338 (2001).
[15] Baker, W. E. and Saleem, M., *Polym. Eng. Sci.*, **27**, 1634–1641 (1987).
[16] Scott, C. E. and Macosko, C. W., *Polymer*, **35**, 5422–5433 (1994).
[17] Fowler, M. W. and Baker, W. E., *Polym. Eng. Sci.*, **28**, 1427–1433 (1988).
[18] Beck Tan, N. C., Tai, S.-K. and Briber, R. M., *Polymer*, **37**, 3509–3519 (1996).
[19] Pillon, L. Z. and Utracki, A., *Polym. Eng. Sci.*, **24**, 1300–1305 (1984).
[20] Pillon, L. Z., Utracki, A. and Pillon, D. W., *Polym. Eng. Sci.*, **27**, 562–567 (1984).
[21] Yin, Z., Koulic, C., Pagnoulle, C. and Jérôme, R., *Macromolecules*, **34**, 5132–5139 (2001).
[22] Schulze, J. S., Moon, B., Lodge, T. P. and Macosko, C. W., *Macromolecules*, **34**, 200–205 (2001).
[23] Scott, C. E. and Macosko, C. W., *J. Polym. Sci. Pol. Phys.*, **32**, 205–213 (1994).
[24] Schäfer, R., Kressler, J., Neuber, R. and Mülhaupt, R., *Macromolecules*, **28**, 5037–5042 (1995).

[25] Schulze, J. S., Cernohous, J. J., Hirao, A., Lodge, T. P. and Macosko, C. W., *Macromolecules*, **33**, 1191–1198 (2000).
[26] Snively, C. M. and Koenig, J. L., *Appl. Spectrosc.*, **53**, 170–177 (1999).
[27] Snively, C. M. and Koenig, J. L., *J. Polym. Sci. Pol. Phys.*, **37**, 2261–2268 (1999).
[28] Ribar, T., Bhargava, R. and Koenig, J. L., *Macromolecules*, **33**, 8842–8849 (2000).
[29] Shull, K. R. and Kramer, E. J., *Macromolecules*, **23**, 4769–4779 (1990).
[30] Lyu, S. P., Cernohous, J. J., Bates, F. S. and Macosko, C. W., *Macromolecules*, **32**, 106–110 (1999).
[31] Shull, K. R. and Kellock, A. J., *Macromolecules*, **23**, 4769–4779 (1990).
[32] Shull, K. R., Kellock, A. J., Deline, V. R. and MacDonald, S. A., *J. Chem. Phys.*, **97**, 2095–2104 (1992).
[33] Jiao, J., Kramwe, E. J., de Vos, S., Möller, M. and Koning, C., *Polymer*, **40**, 3585–3588 (1999).